Romanian Academy
"Petru Poni" Institute of Macromolecular Chemistry

Nr. 4487/3 X 2023

Mrs./Mr. .....

We inform you that on **30th of October 2023, XXX, in** XXX of the Institute of Macromolecular Chemistry "Petru Poni", Iasi, will take place the public presentation of the doctoral thesis "Chitosan derivatives for the development of dressings for wound healing", author **Alexandru Anisiei,** in order to confer the scientific title of doctor.

The doctoral committee has the following composition:

PRESIDENT:
CS I Valeria Harabagiu, PhD
"Petru Poni" Institute of Macromolecular Chemistry, Iasi

DOCTORAL SUPERVISOR:
CS I Dr. Habil. Luminita Marin
"Petru Poni" Institute of Macromolecular Chemistry, Iasi

DOCTORAL CO-SUPERVISOR:
Prof. Dr. Habil. Liliana Mititelu-Tartau
"Grigore T. Popa" University of Medicine and Pharmacy, Iasi

REFEREES:
CS I Dr. Habil. Mariana Pinteala
"Petru Poni" Institute of Macromolecular Chemistry, Iasi

Prof. Dr. Habil Paizs Csaba,
"Babes-Bolyai" University, Cluj

Prof. Dr. Ionel Mangalagiu
"Alexandru Ioan Cuza" University, Iasi

In accordance with the Regulations on the organization and PhD defense within the Romanian Academy, we send you the summary of the doctoral thesis with the kind request to communicate your appreciations and observations. On this occasion, we invite you to participate in the public defense of the doctoral thesis.

ACADEMIA ROMÂNĂ INSTITUTUL DE CHIMIE MACROMOLECULARĂ "PETRU PONI" IAȘI

Director,
Dr. Valeria Harabagiu

Acknowledgements

With honor and joy, I dedicate this doctoral thesis to all those who have supported and encouraged me during the last three years of adventure.

First, I would like to thank **Dr. Luminita Marin**, my scientific supervisor, for guiding me with professionalism, patience, and wisdom. She was a mentor and a role model to me, who not only provided me with academic knowledge and advice, but also confidence and motivation. I would also like to thank **Dr. Liliana Mititelu-Tartau**, without whom the complexity of the studies would not have been the same.

I thank **Dr. Dalila Belei** for the initiation and guidance in the research, starting from my undergraduate studies until now.

I would like to thank the members of the evaluation committee, **Dr. Mariana Pinteala**, **Dr. Csaba Paizs** and **Dr. Ionel Mangalagiu** for participating in this important event in my life and for their suggestions.

I thank the **Romanian Academy** for the financial support provided during the doctoral internship.

I also thank the management of **"Petru Poni" Institute of Macromolecular Chemistry** in Iasi for their support in the elaboration of my doctoral thesis and in my training as a researcher.

I am grateful to my colleagues from **"Petru Poni" Institute of Macromolecular Chemistry** for the beautiful collaboration we had. In particular, I would like to thank my colleagues from the **Polycondensation and Thermostable Polymers** collectives who have always been by my side with help, advice, and encouragement. Thanks to the colleagues from **Intelcentru** department for conducting biocompatibility and antimicrobial activity studies.

Finally, I would like to thank the dearest people in my life: **my family**. I am extremely grateful to my **parents, sister**, and **girlfriend,** who have supported me unconditionally during all these years. They were my source of inspiration, energy, and love.

Table of Contents

Introduction

Chitosan is a biopolymer that is attracting the attention of researchers due to its potential application in various fields, such as agriculture, medicine, and industry. Chitosan is a derivative of chitin, a natural polysaccharide that is abundant in the shells of crustaceans and in the cell wall of fungi. Chitin is the second most abundant polysaccharide on Earth after cellulose and plays a special role in the structure and functions of many organisms.

The history of chitosan can be traced back to the 19th century when chitin was discovered and named by the French chemists Henri Braconnot and Auguste Odier. Since then, chitosan has been studied and modified by many researchers, who have explored its chemical properties. Chitosan was first obtained by Rouget in 1859 by treating chitin with potassium hydroxide, but the name chitosan was first used by Hoppe - Seyler in 1894. Chitosan has been used for various purposes, such as a clarifying agent in winemaking, as a biopesticide in agriculture, as a wound dressing in medicine, and as a coating material in industry. Chitosan is also being investigated for its applications in emerging fields, such as biomedicine, nanotechnology, and biotechnology. Chitosan is a versatile and durable biopolymer that can be adapted to meet diverse needs and challenges.

Electrospinning is a technique for producing nanofibers from solutions or melts of polymers by applying a high electric voltage. Electrospinning has a long history dating back to the 17th century when the movement of liquids by electrostatic force was first observed by William Gilbert. The first patent on electrospinning was filed by John Francis Cooley in 1900, who used a nozzle connected to an electric field to draw fibers from a liquid. In 1914, John Zeleny published a study on the behavior of liquid droplets at the end of metal capillaries, which laid the foundation for mathematical modeling of electrospinning. Since then, electrospinning has been developed and improved by many researchers, who have explored its principles, parameters, and applications.

Electrospinning of chitosan has been widely investigated for its potential applications in various fields, such as controlled drug delivery, tissue engineering, wound healing, and water treatment. Chitosan has many advantages, such as biocompatibility, biodegradability, antimicrobial activity, and low toxicity. However, electrospinning of chitosan is a challenge due to its low solubility and viscosity. Therefore, different strategies have been developed to improve the electrospinning of chitosan, such as blending with other polymers, modifying the molecular structure, adding solvents or additives, and optimizing process parameters.

Electrospinning can modify the properties of chitosan nanofibers compared to the original chitosan solution or bulk material. For example, electrospinning can increase the surface-to-volume ratio of chitosan nanofibers, which can improve their adsorption capacity, bioactivity, and drug release behavior. Electrospinning can also affect the crystallinity, orientation, porosity, and mechanical strength of chitosan nanofibers depending on process parameters such as voltage, flow rate, distance, humidity, and temperature. Electrospinning can also introduce functional groups or nanoparticles into chitosan nanofibers through mixing or coaxial electrospinning methods, which can improve their functionality and performance for specific applications.

Nanofibers of chitosan have been used to develop new wound healing materials and intelligent biomaterials due to their various functionalities, such as reducing swelling, non-toxic nature, biocompatibility, antimicrobial potential, maintaining a moist environment, ability to absorb wound fluid and promote skin regeneration, while also eliminating the risk of infection. Infection is one of the most common complications that can slow down the wound healing process. An infected wound is a localized defect or excavation of the skin or underlying soft tissue in which pathogenic organisms have invaded the viable tissue around the wound. Wound

infection triggers the body's immune response, causing inflammation and tissue damage, as well as slowing down the healing process.

Thus, the PhD thesis entitled "**Chitosan derivatives for the development of dressings for wound healing**" aims to develop bioactive chitosan-based materials that can be used in the treatment of burn wounds. The thesis is structured in seven chapters: **Chapter I** presents literature data on the preparation of chitosan-based materials using the electrospinning method, while **Chapter II** discusses general aspects of wounds. Chapters **III, IV, V** and **VI** present the results of the author's research, and **Chapter VII** includes a presentation of the materials, methods and equipment used to obtain the results.

Chapter I focuses on the presentation of the main pathways reported in the literature for the electrospinning of chitosan, with emphasis on the impact of the parameters used in the electrospinning process and the morphological characteristics of the obtained fibers. The advantages and disadvantages of each pathway are also discussed, as well as the potential applications of the obtained materials.

Chapter II discusses general aspects of wounds, types of wounds, wound healing, and factors that hinder the healing process, with emphasis on burn wounds.

Chapter III aims to obtain chitosan fibers and their functionalization with an aldehyde with bioactive properties. It is structured in three subchapters, the first being dedicated to the argumentation of the design of the proposed material, the second is a preliminary study in which the electrospinning and imination of chitosan were performed to establish the protocol for obtaining the desired material. Subchapter III targets the actual obtaining of chitosan fibers functionalized with 2-formylphenylboronic acid.

Chapter IV focuses on the obtaining of bandages for the treatment of burn wounds caused by scalding, bandages that are based on mesoporous chitosan fibers loaded with the broad-spectrum antibiotic, Norfloxacin, and sealing it in the pores by surface modification via imination with 2-formylphenylboronic acid. In this study, the composition, morphology, and properties of these bandages that are required for wound healing were evaluated.

In **Chapter V**, nanofibrous materials based on quaternized chitosan were obtained. This chitosan derivatives was considered because it has improved properties compared to the starting compound, such as mucoadhesivity, bioadhesivity, antimicrobial and antioxidant properties, making it the ideal candidate for obtaining materials that can be used in tissue engineering. The composition, morphology, and properties of chitosan and quaternized chitosan fibers were investigated, and the biocompatible fibers with an optimal ratio between the two components were investigated in wound healing experiments.

Chapter VI comprises a series of multifunctional materials with the aim of meeting the challenges of high-performance applications. The study focuses on the electrospinning of chitosan/quaternized chitosan nanofibers doped with copper oxide nanoparticles to obtain multifunctional biomaterials with antimicrobial activity. Needle-free electrospinning technology was used for mass production and the characteristics of the resulting nanofibers were evaluated, including mechanical properties, antimicrobial, antioxidant, biodegradability, and particle filtration efficiency.

Chapter VII presents the experimental part that includes the materials and methods used for conducting the studies. In addition, this chapter also presents the methods for preparing chitosan-based fibers.

3.1 Introduction. Argumentation of the proposed design in the context of literature data

Chitosan nanofibers obtained by electrospinning are materials with significant applications in biomedicine, food industry, environmental protection, and electronics, due to their high surface area and remarkable performance (they are biocompatible, biodegradable, and have antimicrobial properties).

One of the promising research areas is the treatment of burn wounds, a major health problem. Chitosan nanofibers, due to their structural similarity to the natural extracellular matrix, are ideal candidates for bandages.

In search of a solution, new multifunctional biomaterials based on microporous chitosan nanofibers, functionalized with an antimicrobial agent, have been proposed. These fibers can improve gas exchange, release antimicrobial agents on demand, and gradually biodegrade in the presence of enzymes from wound exudate, thus avoiding the trauma associated with mechanical removal. This approach could revolutionize wound care, especially burn care, by reducing the risk of infections and accelerating the healing process.

3.3 Microporous chitosan fibers for obtaining biodegradable biomaterials with antimicrobial activity

A series of imino-chitosan nanofibers with a different content of imine units was prepared by heterogeneous condensation reaction of chitosan fibers with 2-formylphenylboronic acid (BA) in ethanol.

The synthesis was performed in different molar ratios between glucosamine units of chitosan and the formyl unit of the aldehyde (**Scheme 11**).

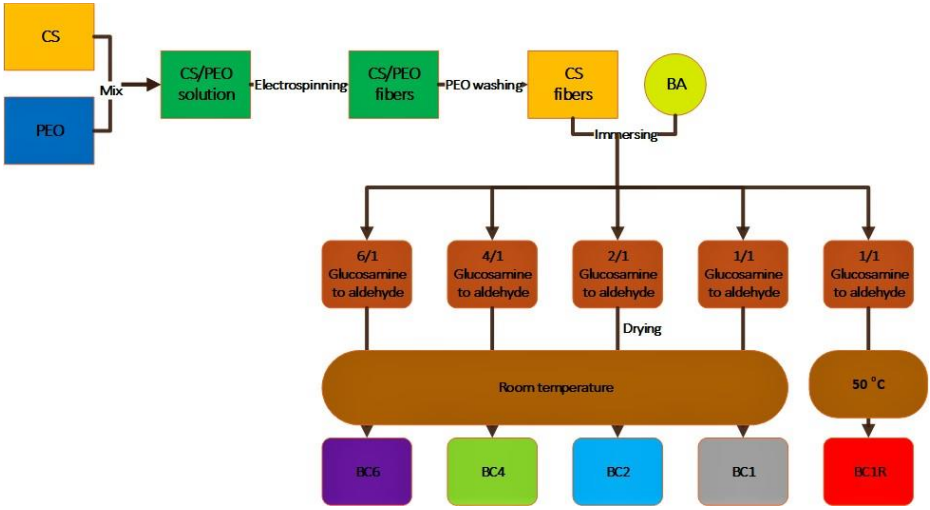

Scheme 11. *Preparation protocol of the imino-chitosan nanofibers*

3.3.1 Structural characterization of imino-chitosan fibers

Imination of chitosan fibers was studied by FTIR, ^{1}H-NMR and UV-Vis spectroscopy.

FTIR spectroscopy demonstrated the formation of imine bonds by the appearance of a characteristic band at 1624 cm^{-1}. The formyl band of 2-formylphenylboronic acid was not observed, indicating that there is no unreacted aldehyde in the functionalized fiber samples.

^{1}H-NMR spectroscopy confirmed the imination reaction and provided quantitative information on the degree of conversion of amino groups to imino units. The degree of conversion increases with increasing the molar ratio of amine to aldehyde and reaches a maximum value of 52.87%.

UV-Vis spectroscopy demonstrated the reversibility of the imine bond. The equilibrium of the imination reaction is shifted towards the formation of reactants as the aldehyde is removed from the system, concluding therefore that the aldehyde is released on demand.

3.3.2 Fibers' morphology

SEM analysis of the electrospun samples from the CS/PEO solution showed a fine fibrillar morphology with no bead defects and a diameter of 137 ± 21 nm. By removing PEO from the fibers, the average diameter was higher than 176 ± 33 nm. By imination, the fibrillar materials became less homogeneous, with an average diameter between 139 ± 14 and 185 ± 28 nm and inter-fibrillar pores around 1 μm and intra-fibrillar micropores up to 2 nm (as demonstrated by water vapor sorption). When the samples were analyzed using polarized light optical microscopy, they showed a continuous birefringent texture, indicating that the chitosan macromolecules aligned during the electrospinning process.

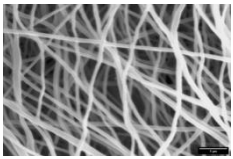

a) **CS/PEO**, 137±21 nm

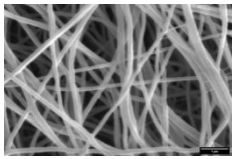

b) **CS**, 176±33 nm

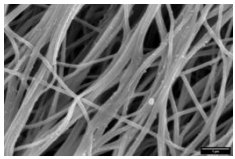

c) **BC1**, 147±18 nm

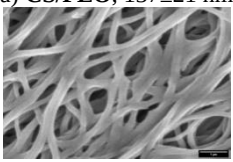

d) **BC1R**, 185±28 nm

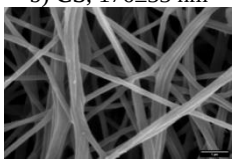

e) **BC2**, 152±21 nm

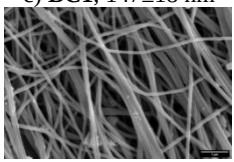

f) **BC4**, 139±14 nm

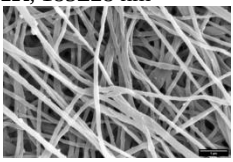

g) **BC6**, 142±22 nm

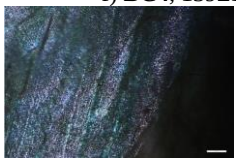

h) **BC1R**

Figure 16*. SEM representative images (a-g) of CS/PEO, CS, and imino-chitosan fibers (1 μm scale), h) POM representative image of* ***BC1R*** *sample (100 μm scale)*

3.3.3 Swelling behavior

Chitosan and imino-chitosan fibers showed rapid swelling in contact with water, reaching a MES of approximately 30 g/g in less than 1 hour. This swelling ability is important for using fibers as bandages in wound healing, as it allows draining the exudate while maintaining a moist environment, necessary for the healing process.

3.3.4 Biodegradation of the fibrillar material

In the first stage of healing, when the pH is 8.5, the biodegradation of the fibers begins, releasing the bioactive aldehyde. Biodegradation intensifies in the second stage of healing when the pH reaches 10, and the fibers break down in the third stage of healing when the pH of the wound reaches 5.5, the pH of healthy dermis. It can be estimated that microporous chitosan fibers should completely degrade during the wound healing period, thus avoiding traumatic debridement.

3.3.5 Antimicrobial activity

The antimicrobial activity of nanofibers was evaluated against representative Gram-positive (*S. aureus*) and Gram-negative (*E. coli*) bacteria, yeasts *(C. albicans*) and fungi (*A. brasiliensis*).

Even though chitosan is well known to have antimicrobial properties [1], chitosan fibers did not inhibit microbial growth in their vicinity. In the case of imino-chitosan fibers (**BC1-BC6**), a zone of inhibition appeared against *C. albicans* (**Figure 23b**), *S. aureus* (**Figure 23c**) and *A. brasiliensis* (**Figure 23d**). The activity of the fibers was directly proportional to the degree of imination of the samples, but a strong activity was observed even for the sample **BC6** which had the lowest degree of imination.

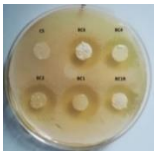

b) *S. aureus*

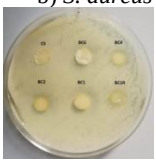

c) *C. albicans*

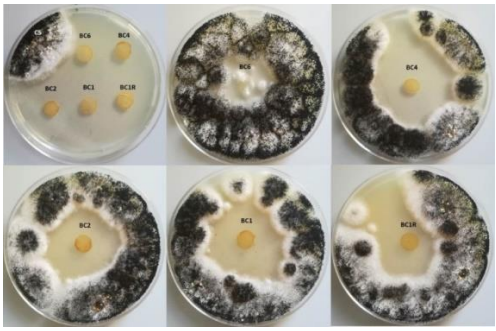

d) *A. brasiliensis*

Figure 13*. Antimicrobial fiber activity against b) S. aureus, c) C. albicans and c) A. brasiliensis strains*

3.3.6 *In vitro biocompatibility*

The results indicated that, except for samples **BC1** and **BC1R**, all samples met the conditions of the biocompatibility evaluation (**Figure 25**). The cytotoxicity of samples **BC1** and **BC1R** was caused by the large amount of imine units on the fibers' surface and is expected to decrease once the amount of aldehyde is consumed in the healing process.

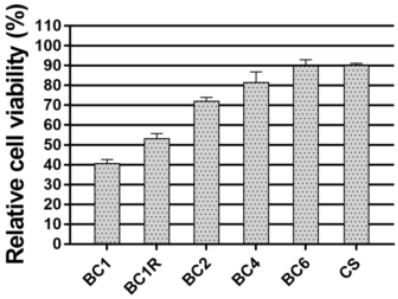

a)

Figure 25*. a) Relative cell viability of NHDF cells (Results are presented as mean ± SEM (standard error of the mean), n = 9)*

3.3.7 Conclusions

The preparation of microporous chitosan nanofibers and their condensation with 2-formylphenylboronic acid with an imination degree of 16% led to the obtaining of biomaterials with (i) the ability to swell and thus drain the wound exudate favoring a moist environment suitable for healing; (ii) biocompatibility and bioadhesion beneficial for tissue repair; (iii) beneficial antimicrobial activity to prevent wound infection in the early stages of healing and (iv) biodegradation rate that matches well with the wound healing period, indicating avoidance of traumatic debridement. All these cumulative properties satisfy the requirements of an ideal dressing and encourage further investigation to provide a marketable product. Moreover, this study brings to the researchers' attention a promising new design for wound dressings consisting of microporous chitosan nanofibers functionalized by imination with antimicrobial agents.

Chapter IV: Chitosan nanofibers with norfloxacin filler for burn healing

4.1 Introduction

The idea of this study was to develop bioabsorbable dressings capable of healing burn wounds. In developing the design of a suitable dressing, the results obtained and presented in the previous chapters were considered. Thus, previous studies have demonstrated that neat chitosan fibers can be obtained by electrospinning a chitosan/PEO solution followed by PEO removal [2–4]. This strategy enriches chitosan fibers with intra-fibrillar pores, which bring additional advantages such as high absorption capacity and high biodegradation rate. Another interesting aspect is the functionalization of chitosan through reversible covalent imine bonds, and it was demonstrated that materials with dynamic properties are obtained, able to respond to external stimuli such as pH or components' consumption [2,3,5]. In this way, by conducting the imination reaction with an aldehyde that exhibits antimicrobial properties, materials capable of releasing the antimicrobial aldehyde "on demand" can result, by shifting the equilibrium of the imination reaction toward the reactants as the aldehyde is consumed in the pathogen inactivation process [6]. Thus, in this context, mesoporous chitosan fibers loaded with a broad-spectrum antibiotic, Norfloxacin, modified on the surface by imination with an aldehyde with antimicrobial activity, 2-formylphenylboronic acid (AB), were obtained. The materials were investigated in detail, considering their composition, morphology, and properties necessary for wound healing.

4.2 Preparation of chitosan-based dressings and their composition

Composite nanofibers were obtained in three stages.

(1) Mesoporous chitosan (**C**) fibers were obtained by electrospinning a CS/PEO solution followed by removal of PEO. Thus, the CS/PEO solution (2/1, m/m) with a concentration of 2,1 % in 80 % acetic acid was electrospun using electrospinning parameters: voltage = 7 kV, flow rate = 0,4 mL/h, needle-collector distance = 10 cm, inner needle diameter = 0,8 mm, rotating collector rotation speed = 800 rpm, temperature = 27 – 28 °C. The PEO was removed by washing the fibers with a solution of NaOH (5 %) to neutralize residual acetic acid and washing with water to pH neutral. In order to preserve the intra-fibrillar pores created, the fibers were then freeze-dried from the wet state.

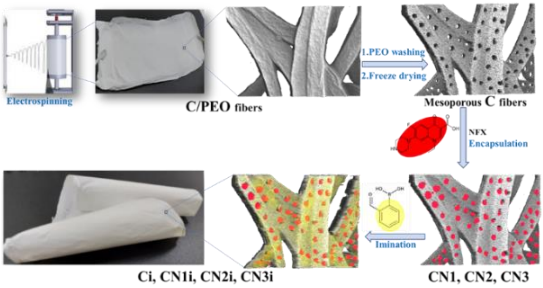

***Scheme 12**. Pictorial representation of the preparation pathway of the studied composite fibers*

(2) The NFX loading step was performed by the equilibrium adsorption method by immersing the fibers in a saturated norfloxacin solution using different loading conditions and incubating them for 24 hours in Plexiglass flasks. After this, the fibers were dried under atmospheric conditions and then under vacuum.

(3) The surface modification step of the fibers was performed by spraying the samples with a 0,28 % AB solution so that the molar glucosamine/aldehyde ratio was 10/1.

The design of the composite fibers (**Scheme 12**) was demonstrated by thermogravimetric analysis (TGA), dynamic vapor sorption (DVS), FTIR spectroscopy and ^{1}H-NMR.

FTIR and ^{1}H-NMR spectra revealed the efficiency of drug loading and imination of chitosan fibers, but also provided information on the physical interactions between the components. Thus, the FTIR spectra confirmed the encapsulation of NFX by the appearance of the characteristic bands: the stretching vibration bands of the carbonyl group at 1636 cm^{-1} and the shearing bands of the quinolinic NH at 1618 cm^{-1}. The imination of the fibers with AB was confirmed by FTIR spectra, which showed the appearance of a characteristic vibrational band at 1625 cm^{-1}. Regarding the NMR spectra, the encapsulation of NFX in the fibers led to the broadening of the characteristic signals and their displacement from 8.52 - 6.94 ppm to 8.9 - 7.2 ppm, in accordance with the modification of the chemical neighborhoods through the appearance of intermolecular hydrogen bonds with the macromolecules of chitosan.

4.3 Morphological characterization

SEM images showed the formation of continuous fibers with an average diameter of about 170 nm, entangled to form a super porous material with micro- and submicro-pores with diameters up to 4 μm. Comparison of SEM images with high magnification (100,000x) revealed a rougher topography of NFX-loaded fibers, but no drug crystals were detected, supporting the hypothesis of drug encapsulation inside them. The strong birefringence of fibers under polarized light indicates a degree of crystallinity, resulting from the electrospinning process due to the alignment of macromolecules in the electric field [7].

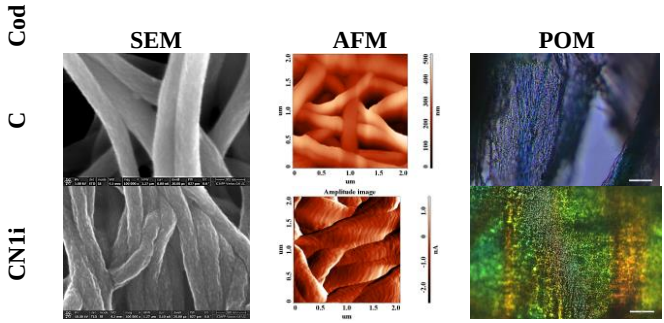

Figure 27. *SEM, AFM and POM images of the studied samples*

4.4 Behavior of the fibers in wet environment. Swelling, biodegradation and *in vitro* drug release

When the fibers are immersed in an environment with the characteristic pH for the first stage of wound healing (pH=7.4-10), the **C** fibers swell rapidly, reaching a swelling degree of about 17 g/g, in less of 15 minutes (**Figure 29a**). When they are loaded with NFX, the average fiber adsorption decreases to a value of about 7 g/g, and further decreases after imination to a value of about 5 g/g (**Figure 29a**).

The fibers showed a controlled release of NFX for 8 hours, the release being correlated with the pH of the environment: for a higher pH, a higher release rate was recorded, due to the better solubility of norfloxacin in alkaline pH (**Figure 29b,c**). It was observed that imination of the samples slowed down the release of the drug. For example, for sample **CN1** a release of 66 % was obtained after 4 hours, and for sample **CN1i** a release of norfloxacin of 53% was recorded.

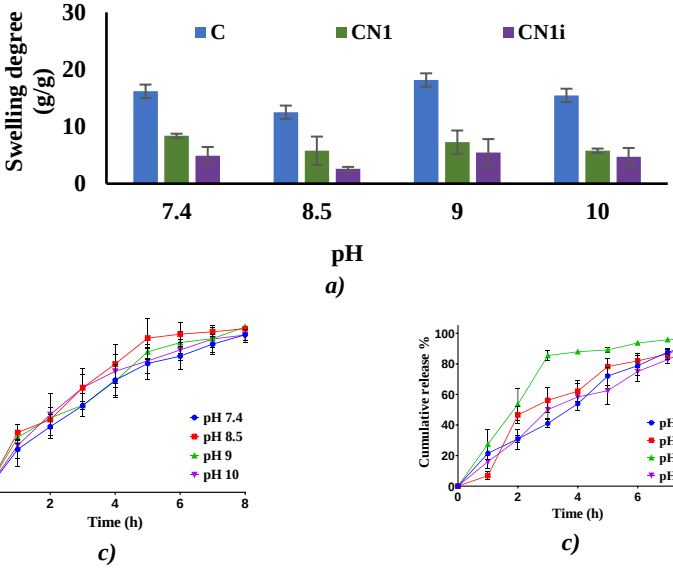

Figure 29. *Samples' behavior in wet environment: a) The swelling degree in media of different pH, exemplified on **C**, **CN1**, and **CN1i** samples; and in vitro drug release in media of different pH for b) **CN1** and c) **CN1i***

4.5 Antimicrobial activity

The antimicrobial activity was determined on microbial strains representative for infected wounds, Gram-negative and Gram-positive bacteria, as well as yeast and fungal strains. The comparative analysis of the results showed that the composite samples have strong antimicrobial activity with a broad spectrum of action against all studied pathogens, resulting from the contribution of each component. Thus, the weak activity of pure chitosan fibers (**C**) against *E. coli* and *K. pneomonaiae* was enhanced with antimicrobial properties against *S. aureus*, *E. faecalis* and *P. aeruginosa* when the fibers were loaded with NFX (**CN1**) and with activity against *C. glabrata* and *A. brasiliensis* when the fibers were iminated with **AB** (**Ci, CN1i, CN2I**). Antimicrobial activity increased with increasing amount of NFX (**CN1i** *vs.* **CN2i**).

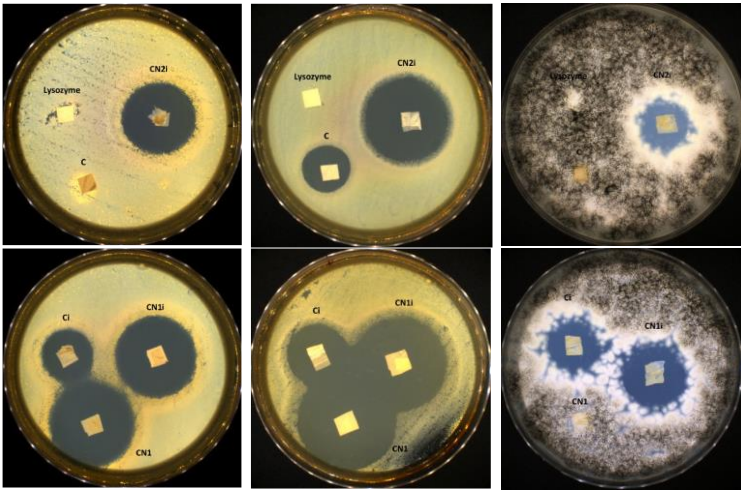

S. aureus *E. coli* *A.brasiliensis*

Figure 31. *Representative images of areas of inhibition developed by samples studied against representative strains after 24 hours incubation (for bacteria and yeast strains) and 72 hours (for fungal strains)*

4.6 In vitro biocompatibility

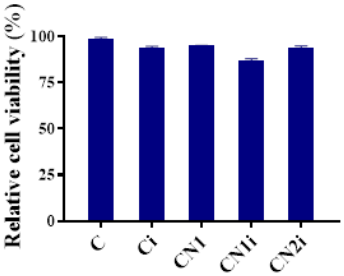

The results showed that the cell viability was higher than 85% for all samples, exceeding the 70% threshold for medical devices used in contact with living tissues (**Figure 32a**).

Figure 32. *Graphical representation of relative cell viability of NHDF cells after 48 h contact with the studied samples, compared to untreated cells. Results are presented as mean ± standard error of the mean (S.E.M.), n = 9*

4.7 *In vivo biocompatibility*

The impact of the samples on living tissue was investigated *in vivo* in rats by evaluating biochemical parameters that provide information on the clinical stage and metabolic function of organs and tissues.

Biochemical and histopathological evaluation shows that subcutaneous administration of samples did not cause damage during biodegradation and blood circulation of sample residues.

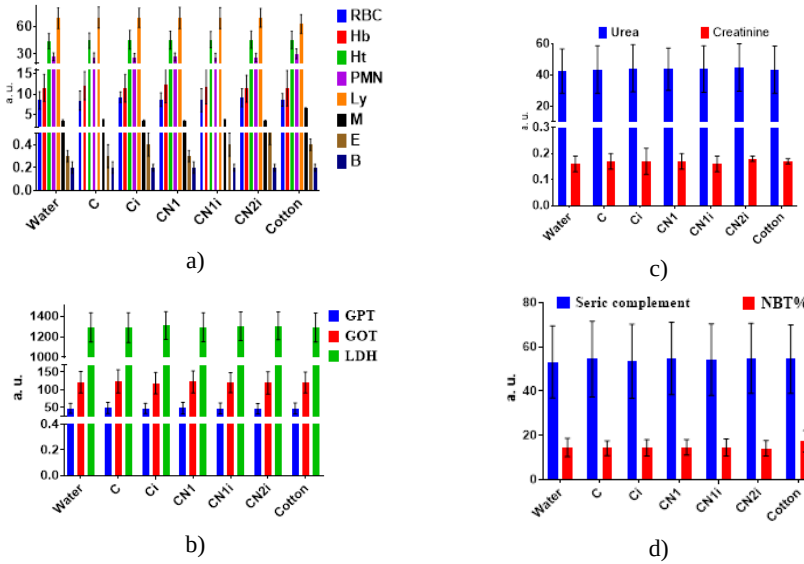

Figure 33. *Level of a) hematological parameters; b) end products of metabolism; c) plasma enzymes and d) immunological parameters, measured 24 hours after subcutaneous implantation of samples in rats*

4.8 Wound healing

The wound healing study evaluated the ability of the fibers to heal deep dermal wounds in rats over a 25-day period. Macroscopic parameters (appearance, surface, eschar, epithelialization) and microscopic criteria (coagulation, cell layers, angiogenesis, inflammatory cells, fibrin deposits, epithelialization) were analyzed. A gauze and vaseline dressing were used as control groups. Images of the burns were documented at different time stages. It is noteworthy that the mesoporous chitosan fibers used in the study demonstrated faster healing than other chitosan-based fibers such as chitosan/PEO. This difference can be attributed to the absence of PEO and the presence of mesopores within the fibers, which facilitate rapid swelling and moisture favorable for wound healing.

The comparative wound healing study showed that the use of chitosan nanofibers promotes faster healing and intense fibrillar synthesis. Chitosan nanofibers function as an active factor in wound healing, interacting directly with the wound, unlike gauze, which has a more passive protective role.

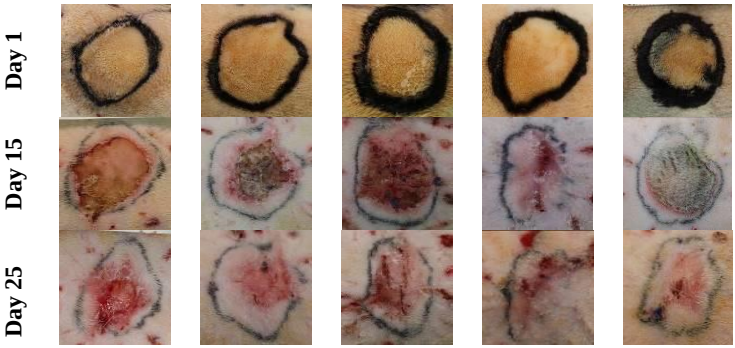

Figure 35*. Wound appearance on days 1, 15 and 25 of the positive control groups and the studied samples. The tattoo persisted for all lesions (except one, which did not interfere with the outline, making the line clearly visible during digital measurements)*

At the end of the study, **CN2i** performed superiorly in the maturation and epithelialization stage with reduced inflammation, followed by **Ci** and **CN1i**. Group **C** showed late inflammation and slower but still faster development than the gauze control group. The reduced mobility of chitosan chains in the exudate influenced the evolution of group **C**. In contrast, **CN1i** and **CN2i** showed a consistently more favorable response.

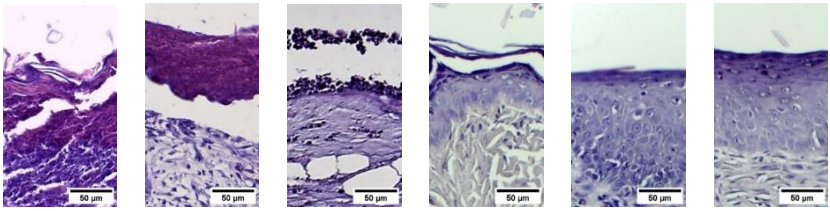

a) Control, day 1 **b) Gauze, day 25** **c) C, day 25** **d) Ci, day 25** **e) CN1i, day 25** **f) CN2i, day 25**

Figure 35. *Wound healing score and representative histological images on tissue samples collected on day 1 of wound onset (a) and on day 25 of healing in the case of application of b) gauze, c)* ***C****, d)* ***Ci****, e)* ***CN1i*** *and f)* ***CN2i***

The results of this study pave the way for further research in the field of burn wound healing. Understanding the interaction of chitosan nanofibers with the complex physiological processes of wound healing may bring new insights into the development of novel dressings.

4.9 Conclusions

In this study, mesoporous chitosan nanofibers loaded with norfloxacin and coated with an antifungal agent *via* imino linkages were developed. The fibers were evaluated for their applicability in treating wounds such as burns. The fibers had a porous structure, which allowed them to swell quickly and retain moisture. This makes them suitable for treating wounds, as moisture is essential for healing. Composite materials passed biocompatibility tests and did not show harmful effects on laboratory animals. Burn wound healing experiments have shown that mesoporous chitosan fibers promote early fibrillar synthesis. The addition of the antifungal agent improves tissue regeneration by inhibiting the growth of pathogens. Loading the fibers with norfloxacin and sealing them with the antifungal agent resulted in complete wound closure and extensive re-epithelialization. In conclusion, the use of mesoporous chitosan nanofibers loaded

with norfloxacin and coated with an antifungal agent through imino linkages proves beneficial in accelerating the wound healing process and improving the quality of newly formed skin. This ternary composite shows potential for medical applications in wound treatment.

Chapter V: Biodegradable Chitosan/Trimethyl Chitosan Nanofibers for Application as Bioabsorbable Dressings for Wound Closure and Healing

5.1 Introduction

Functionalization of chitosan with quaternary ammonium groups, by converting amino groups into quaternary salts, e.g. trimethyl chitosan (TMC), or by grafting side spacers bearing quaternary units, e.g. *N*-(2-hydroxy)propyl-3-trimethyl ammonium chitosan (HTCC), is beneficial for improving the properties of chitosan, such as mucoadhesiveness, bioadhesiveness, antimicrobial, anticoagulant, antioxidant and immunomodulatory properties, making chitosan more suitable for tissue engineering and transdermal drug delivery [8–10]

Efforts have been directed towards the development of an electrospinning procedure of a CS/TMC/PEO ternary blend, in which the PEO plays the role of a sacrificial additive, which is removed to yield biodegradable CS/TMC fibers. The design was chosen considering the improved properties of TMC *vs.* chitosan, but also the fact that pure TMC, due to the high degree of quaternization, can induce a degree of toxicity [10]. It was hypothesized that by combining TMC with chitosan, the benefits of TMC would be preserved while the cytotoxicity would be decreased to an acceptable level for biomedical devices. The composition, morphology, and properties of CS/TMC fibers were investigated, and biocompatible fibers with an optimal CS/TMC ratio that led to a progressive rate of biodegradation were investigated in wound healing experiments.

5.2 The obtaining of chitosan/trimethyl chitosan binary fibers and their structural and morphological characterization

CS/TMC binary fibers were prepared by electrospinning a CS/TMC/PEO ternary solution with 20% (w/w) PEO content and different CS/TMC ratios, followed by selective removal of PEO by successive washings with ethanol (**Scheme 13**).

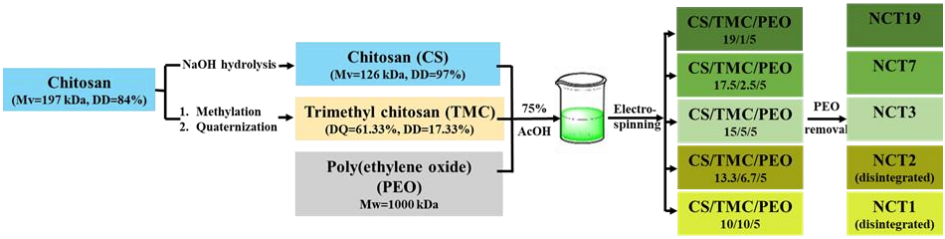

***Scheme 13**. Representation of the preparation of the binary TMC/CS fibers*

The presence of the two biopolymers in binary fibers, CS and TMC**,** was confirmed by FTIR and ^{1}H-NMR spectroscopy, which revealed the presence of all bands characteristic of the two components (**Figure 38b,c**Eroare! Fără sursă de referință.). Thus, the FTIR spectra of CS/TMC fibers revealed an absorption band around 1461 cm^{-1} characteristic to the asymmetric stretching vibration of the C-H bond of the methyl group a -N(CH$_3$)$_3$. The ^{1}H-NMR spectrum revealed TMC-specific chemical shifts from 4.2 to 4.5 for H6'-H2' protons in -N(CH$_3$)$_3$ substituted glucosamine units and 3.5 to 4 ppm and 3.1 ppm for H6-H3 protons and H2 protons in non-N(CH$_3$)$_3$ glucosamine units, respectively, 3.31 ppm for N(CH$_3$)$_3$ protons, and 3.03 ppm for -N(CH$_3$)$_2$ protons.

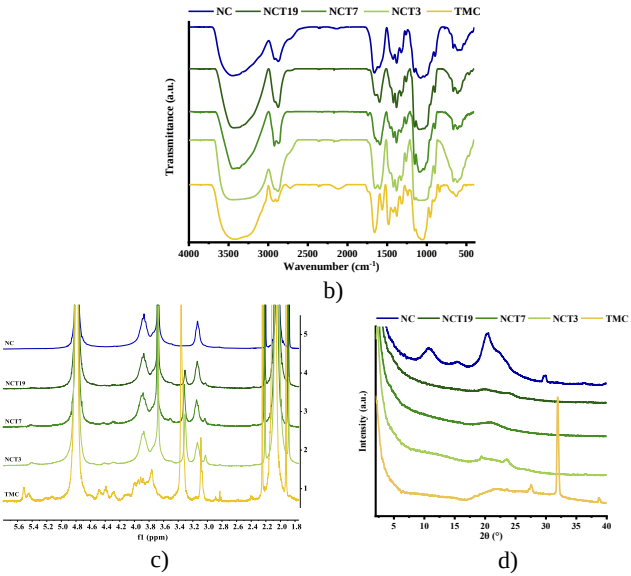

Figure 38*. Characterization of binary fibers by b) FTIR, c) [1]H-NMR and d) XRD*

X-ray diffraction of CS/TMC fibers showed only a broad band of weak intensity with the maximum around 21 º, indicating that the fibers are amorphous, while NC and TMC showed sharper diffraction bands according to some degree of crystallinity (**Figure 38d**), suggesting that the physical forces between CS and TMC caused a random entanglement of their chains, preventing alignment during electrospinning.

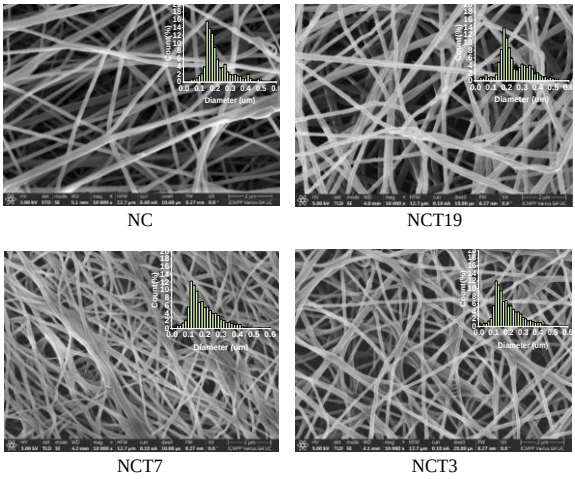

Figure 39. *SEM images of NCT binary fibers and NC reference. Inset: distribution histograms of fibers' diameter*

Fibers with good integrity were obtained for low TMC content (**NCT19**, **NCT7**, **NCT3**), while those with high content (**NCT1**, **NCT2**) partially disintegrated in ethanol during the PEO removal process, which is why they were excluded from the study. The images obtained by SEM analysis showed that **NCT19**, **NCT7** and **NCT3** are smooth-surfaced fibers without defects, while **NCT1** and **NCT2** fibers recovered after ethanol removal showed bead-like defects (**Figure 38**).

5.3 Behavior of fibers in aqueous environment. Solubility, swelling, biodegradation, water vapor sorption

In terms of swelling, the samples reached a maximum degree of swelling, with statistically significantly higher values ($p<0.05$) for samples **NCT3** and **NCT7** in water, which reached a maximum of 35 g/g. The liquid retention capacity slightly decreased over time, remaining high after 24 h of the experiment, with statistically insignificant differences in the degree of swelling between the samples, around 20 g/g in water and 12 g/g in PBS.

Enzymatic degradation, monitored in lysozyme solution in PBS (pH=7.4) for 7 days, showed an increase in the rate of biodegradation along with increasing **TMC** content, reaching statistically significantly higher values of weight loss in compared to chitosan fibers (23% - 44% versus 10%) (**Figure 42c**). In an environment that mimics the evolution of exudate's pH during wound healing, a weight loss of around 20% occurred in the first 4 days, increased slightly to 22% by day 14, and increased sharply to 100% on day 17 (**Figure 42d**).

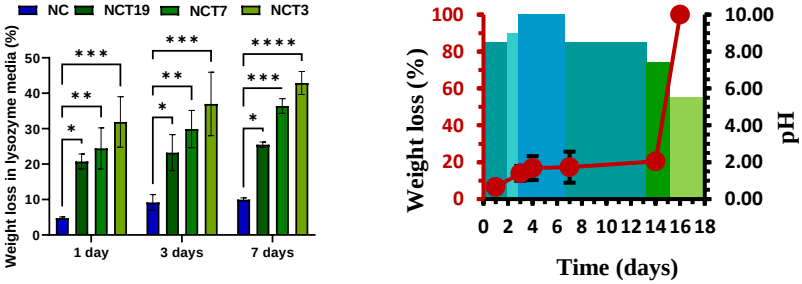

c) d)

Figure 42**. Enzymatic biodegradation in c) lysozyme solution (376 U/ml) in PBS and d) lysozyme media mimicking exudate pH during wound healing exemplified for sample **NCT7

5.5 *In vitro* antimicrobian activity

Antimicrobial activity was investigated against *S. aureus* and *E. coli* strains, representative for Gram-positive and Gram-negative bacteria strains. The investigations were conducted in environments that mimic wound exudate, in the presence of lysozyme which was used as a control. All samples containing TMC were highly effective against *E. Coli* with an inhibition zone for **NCT3** up to 32 mm, and samples **NCT7** and **NCT3** were also effective against *S. aureus*.

Table 12. Antimicrobial activity of tested compounds against reference strains (mm)

Strains	**Inhibition zone (mm)**				
	C	**NC**	**NCT3**	**NCT7**	**NCT19**
Staphylococcus aureus ATCC25923	-	-	15.50 ± 0.15	19.93 ± 0.17	-
Escherichia coli ATCC25922	-	-	31.85 ± 0.21	28.80 ± 3.39	26.90 ±3.96

5.6 In vitro and *in vivo* biocompatibility

The viability of normal human dermal fibroblasts (NHDF) in contact with the studied samples was investigated by the MTS test, for 24 hours, in accordance with the ISO standard for medical devices (**Figure 45**) [11].

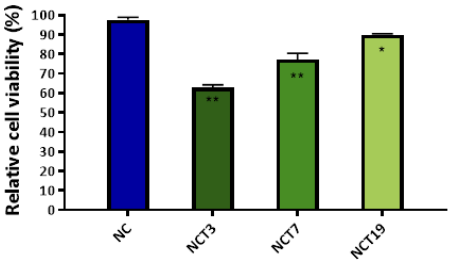

Figure 45. *Biocompatibility of the nanofibers. Data are presented as mean ± S.E.M. (standard error of the mean), n = 9; ** p ≤ 0.0001 (NC vs NCT3; NC vs NCT7), * p < 0.05 (NC vs NCT19)*

Fibers' implantation did not cause any statistically significant deviation of biochemical parameters relevant to the clinical state and metabolic activity of organs and tissues. Thus, hematological parameters: hemoglobin (Hb), hematocrit (Ht), red blood cells (RBC) and white blood cells: polymorphonuclear neutrophils (PMN), lymphocytes (Ly), erythrocytes (E), monocytes (M) and basophils (B) had values similar to those of the negative control indicating that the biodegradation products of the samples that reached the blood did not alter the oxygen carrying capacity and did not induce toxic stress [12]. In addition, the lack of change in the level of eosinophils and basophils indicated that the implanted samples did not trigger allergic reactions.

5.7 Wound healing

The ability of **NCT7** fibers to promote wound healing was investigated in deep (second/third degree) burn models in rats, compared to a standard non-adherent dressing of Vaseline-impregnated gauze (**G**) used as a negative control and sulphadiazine-soaked gauze (**G-SFT**) as a positive control, for a period corresponding to the first wound closure (**Figure 14**). After 22 days of experiment, the mean percentage of wound closure of sample **NCT7** was 49%, for **G-SFT** it was 22% and for **G** it was 19%.

In the tissue samples of the wound covered with sample **G** (**Figure 49**), histological observation revealed a layer of exudate covering the surface of the wound (orange box) and abundant leukocyte infiltration was observed under this layer. In **G-SFT** and **NCT7** samples, epithelial restoration was evident, but while in G-SFT it was observed under a layer of exudate (above the green frame), in **NCT7** the epithelia had a fully functional appearance with the presence of the cornified layer superior protector. In the case of the positive control and the fiber sample, leukocyte infiltration was present beneath the epithelium, suggesting active wound healing. The epithelium of untreated control rats was shown as a comparison term to demonstrate the thickness of the undamaged epithelium.

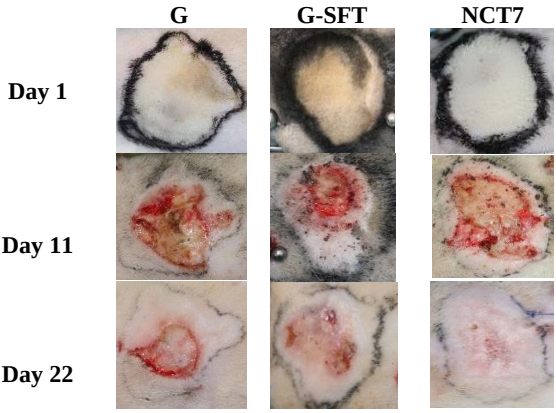

Figure 49. *Burn appearance after infliction (day 1) and on days 11 and 22 of negative (G) and positive control (G-SFT) and NCT7 groups. The wound had 2.5 cm diameter and outlined with a tattoo for easy monitoring of the wound closure percent.*

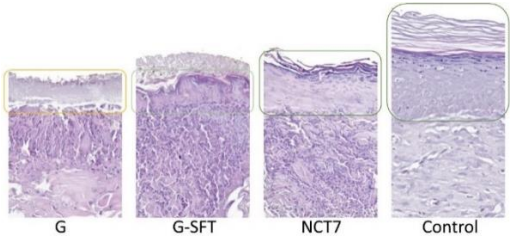

Figure 50. *Histological analysis of tissue samples at day 11. Epithelial formation is shown in green rectangle. The exudate covering the wound is enclosed in an orange rectangle. Objective: 60x 0.9 NA WI*

Like the previous study, NCT7 fibers were loaded with NFX and sealed by imination with AB and assessed for wound healing ability. As expected, the presence of the broad-spectrum drug and the antifungal agent favored a favorable healing process compared to the control NCT7 fiber.

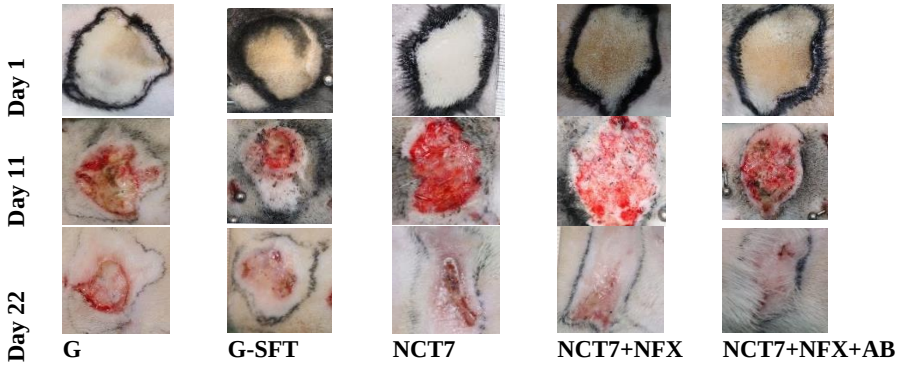

Figure 51. *Burn image after day 1 and on days 11 and 22 of negative (G) and positive control (G-SFT), NCT7, NCT7+NFX and NCT7+NFX+AB groups. The wound was 2.5 cm in diameter and was outlined with a tattoo for easy monitoring of the percentage of wound closure. The tattoo was persistent, thus allowing clear visualization of the outline during digital measurements*

5.8 Conclusions

The study reports for the first time the obtaining of chitosan/trimethyl chitosan nanofibers, by a strategy involving the use of PEO as co-spinning agent and sacrificial additive. This approach provided new biocompatible materials with a particular morphology consisting of mesoporous nanofibers, which favored the adsorption of liquids and their donation to the environment. This approach provided new biocompatible materials with a particular morphology consisting of mesoporous nanofibers, which favored the adsorption of liquids and their donation to the environment. They are gauze-like materials that can be easily handled without any damage, with mechanical properties similar to living tissues. Compared to chitosan fibers, they showed improved biodegradation, controlled by TMC content and environmental pH. The TMC endowed the materials with improved muco- and bioadhesion, and antimicrobial activity against Gram-positive and Gram-negative pathogens. A percentage of 13% TMC in chitosan fibers was shown to lead to biocompatibility in vitro on normal human dermal fibroblasts in accordance with that regulated by standards for biomedical devices, while in vivo tests on experimental rats showed that they did not it affects the clinical condition and metabolic activity of organs and tissues and does not cause any allergenic effect or immune system response. Moreover, the fibers with the best balance of properties promoted total closure and active healing of second-/third-degree burn wounds in rats, with total biodegradation within 11 days, indicating the potential to function as effective bioresorbable dressings.

Chapter VI: Chitosan Nanofibers and Quaternized Chitosan Encapsulating Copper Oxide Nanoparticles

6.2 Design. Morphology and composition

In this study, nanocomposite fibers based on a mixture of polymers (chitosan, HTCC and PEO) and CuONPs nanoparticles were obtained. The fiber composition was designed to combine the beneficial properties of each component:

- Chitosan is a biocompatible and biodegradable matrix that can anchor nanoparticles through dative bonds.
- HTCC has high antimicrobial activity and a stabilizing effect on metal-based nanoparticles.
- PEO is an electrospinning additive, a surfactant for nanoparticles and can improve the mechanical properties of fibers.
- CuONPs nanoparticles have strong antimicrobial and antiviral activity and can improve the electrospinning process by improving conductivity.

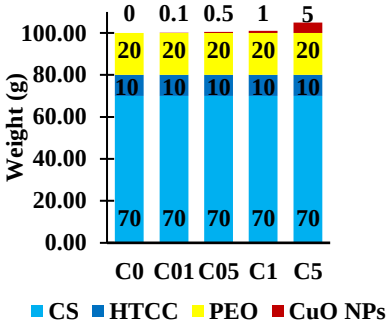

Figure 52. *Graphical representation of the composition of the studied fibers*

The nanocomposite fibers were obtained by electrospinning, this process leading to a fine dispersion of the nanoparticles in the fibers, which is important to obtain improved properties.

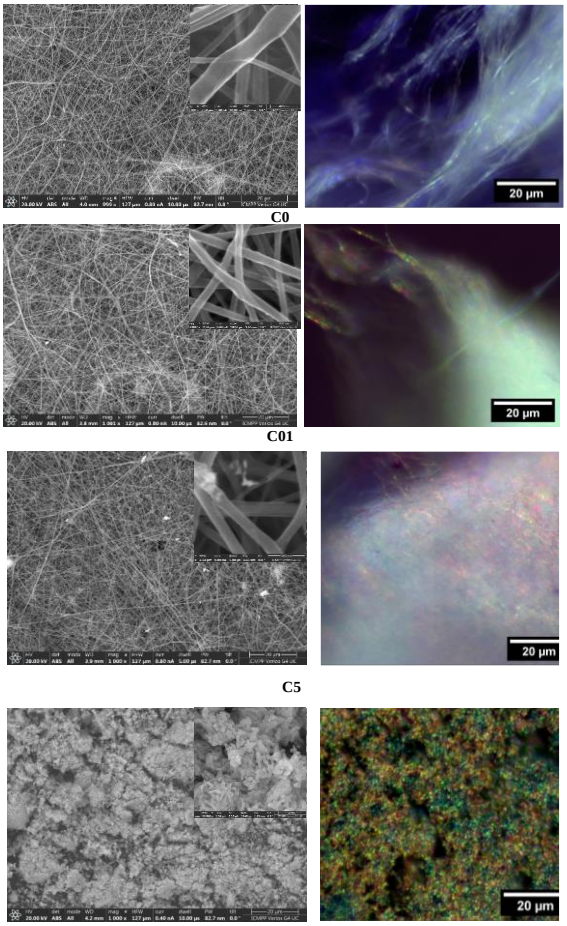

Figure 53. *SEM and POM images of the studied samples (Scale bar in the insert images: 400 nm)*

Defect-free fibers were obtained for all compositions with no mass loss during the electrospinning process. The surface of the fibers was smooth, without obvious agglomerations of nanoparticles, indicating a fine distribution of them inside the fibers (**Figure 53**). Furthermore, data from FTIR and ^{1}H-NMR spectra demonstrated the presence of the three polymers.

A much more in-depth picture of the state of the components in the nanocomposite fibers was brought by X-ray diffraction (**Figure 58a**). The X-ray diffractogram of the CuONPs nanoparticles showed sharp Bragg reflections in the range 32.6 - 75 º, with two very intense bands at 35.5 º and 38.8 º. In contrast, the fibers showed a broad diffraction with two peaks sharp at 19.3 and 23.5 º, which are characteristic of the crystalline phase of PEO [15]. Evidence of CuONPs

stabilization in the polymer blend was provided by the UV–vis absorption spectra of the thin films prepared from the electrospinning solutions compared to the spectrum of the CuONPs suspension in water (**Figure 58b**). Both films and suspensions showed an absorption band at around 259 nm, characteristic for CuONPs, confirming that the nanoparticles did not undergo changes in the electrospinning solutions [16–20].

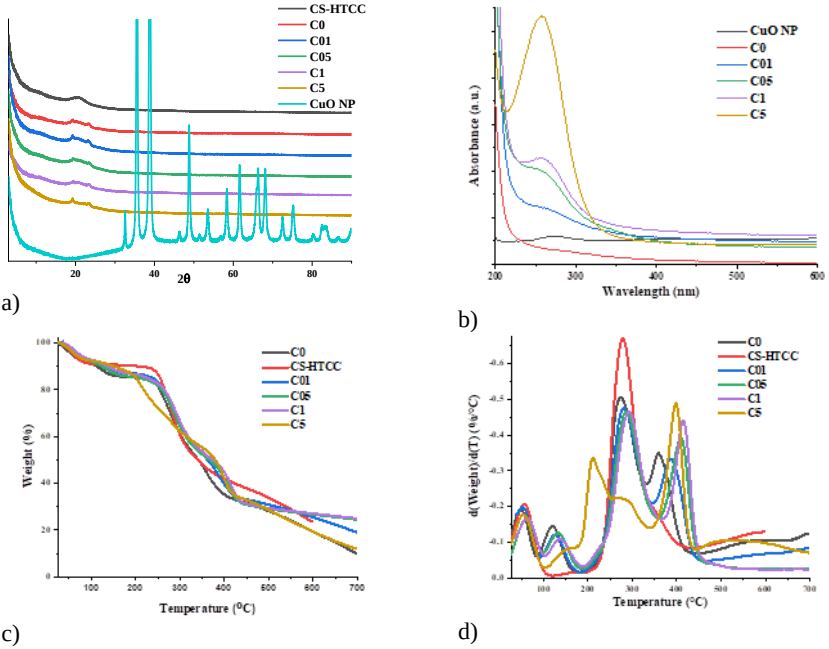

Figure 58. *a) X-ray diffractograms, b) UV-vis spectra, c) TGA and d) DTG curves*

The influence of CuONPs nanoparticles on the mechanical properties of the fibers was evaluated by analyzing a series of parameters: tensile stress, elongation at break and Young's modulus.

The results showed that the tensile stress of the fibers increased with increasing CuONPs content, from 5 to 10 MPa. This increase in tensile strength was attributed to the strong forces developed between the nanoparticles and the polymer matrix. In contrast, the elongation at break decreased with increasing the CuONP content. This reduction in elasticity was caused by fibers' stiffening and structural discontinuities induced by the ordered clusters formed around CuONPs and PEO crystals. Young's modulus, which measures the elasticity of fibers, also increased with increasing CuONP content.

6.5 Antimicrobial activity

All tested samples showed very high antibacterial activity against the Gram-positive bacterial strain represented by *S. aureus* and also against the Gram-negative bacterial strain represented by *K. pneumoniae*, reducing the cell viability with more than 85% (**Figure 62**).

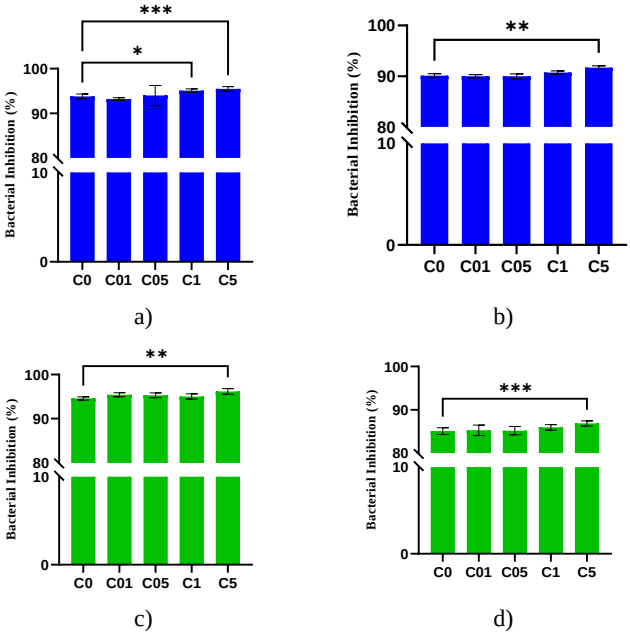

Figure 62. *Bacterial inhibition of strains a,b) S. aureus (blue) and c,d) K. pneumoniae (green) when in contact with fibers of 2x2 cm^2 (a,c) and 0,5x0,5 cm^2 (b,d), respectively (*p <0,05; **p <0,01; ***p <0,001)*

6.6 Permeability/Breathability and dust removal ability

The rate of water vapor penetration through the nonwoven fibers under static conditions was recorded over 7 days. After the first 24 hours, the permeability was high, around 750 g/m^2 day, regardless of the CuONPs content.

In terms of air permeability, **C01** fibers showed similar values to those of **C0**, around 3.6 m^3/m^{2}min, and decreased to about 0.67 m^3/m^{2}min for **C5** fibers with a maximum content of 5% CuONPs. This performance is comparable to that of other chitosan-based nanofibers or nanofibers based on synthetic polymers such as polyurethane, polyvinyl alcohol or polyamide [21–24].

Determination of the filtration efficiency of particles of 2.5 μm (PM2.5) and 10 μm (PM10) revealed values of approximately 62 % and 80.57 % respectively. The values increased slightly with increasing CuONPs content, in agreement with the decrease in fibers' diameter and, consequently, of the inter-fibrillar pores. In all cases, the particle count in the clean room was less than 3% and 1.5%, respectively, compared to 100 % in the polluted room. As expected, the filtration capacity was improved by increasing the nonwoven thickness, reaching 65 % and 90 %, respectively, for sample **C5**, values comparable to those of the filter material in PFE masks.

6.8. Soil biodegradation

Chitosan is known as a biodegradable polymer, whose decomposition products are soil fertilizers [25]. The influence of the chemical composition of the studied fibers on their decomposition was investigated by a soil burial test. Copper oxide nanoparticles delayed the decomposition in a dose-dependent manner. Thus, while samples **C0**, **C01** and **C05** completely disintegrated and absorbed into the soil by day 7, sample **C1** disappeared by day 8, while **C5** completely disappeared after 15 days. This is in close correlation with the higher density of strong intermolecular forces developed by CuONPs.

6.9. Conclusion

In this study, a new method was developed to incorporate copper oxide nanoparticles (CuONPs) into chitosan-based nanofibers. The resulting nanofibers have improved mechanical, antioxidant, antimicrobial and filtration properties. SEM measurements showed that the CuONPs thinned the fibers from 270 to 126 nm. The successful incorporation of CuONPs was demonstrated by EDAX, UV-vis, FTIR, ^{1}H-NMR and TGA analyses. X-ray diffraction indicated the semicrystalline nature of the fibers. CuONPs improved the mechanical properties of the fibers, reaching values of tensile strain up to 10 MPa and Young's modulus of 270 MPa. Quaternized chitosan and CuONPs improved the antioxidant activity of the fibers by reducing free radicals. The fibers exhibited strong antimicrobial activity, reducing Gram-positive *S. aureus* and Gram-negative *K. pneumoniae* by up to 96%. The fibers have a good water vapor transmission rate and air permeability. They also have a PM2.5 and PM10 fine particle removal efficiency comparable to that of synthetic nanofibers. The fibers are biodegradable, with approximately 40% biodegradation in 21 days. These results suggest that CuONPs/chitosan/quaternized chitosan/PEO nanofibers could be used to develop a wide range of products, including dressings, masks, and air filters.

General conclusions

The PhD thesis entitled "**Chitosan derivatives for the development of dressings for wound healing**" has 282 pages divided into seven chapters including 43 tables, 90 figures, 14 schemes and 400 bibliographic notes. The thesis was structured in two parts, a literature study which is represented by **Chapters I** and **II**, and the part of personal contributions (**Chapters III-VII**). The thesis ends with a series of general conclusions.

The original results are presented in five chapters and include:

- Obtaining of chitosan fibers and their functionalization with 2-formylphenylboronic acid
- Obtaining of chitosan-based dressings loaded with norfloxacin and sealed with 2-formylphenylboronic acid
- Obtaining of dressings based on chitosan and trimethyl chitosan
- Obtaining of multifunctional materials based on chitosan and quaternized chitosan encapsulating copper oxide nanoparticles

The following conclusions were drawn from these studies:

1. Preliminary study to obtain chitosan fibers and their functionalization with 2-formylphenylboronic acid.
   - Chitosan fibers were obtained by using poly(ethylene oxide) as co-spinning agent and sacrificial matrix. Binary solutions of chitosan and poly(ethylene oxide) in concentrated acetic acid were electrospun and the obtained binary fibers were successively washed with a solution of NaOH and water in order to neutralize the residual acetic acid and remove the synthetic polymer.
   - The fibrillar morphology and porosity of the obtained materials were demonstrated by scanning electron microscopy and atomic force microscopy.
   - Imino-chitosan fibers were obtained by the heterogeneous system imination reaction of porous chitosan fibers with an aldehyde with anti-pathogenic properties.
   - The degree of conversion of amino groups from chitosan into imine units varied according to the polarity of the solvent used for the preparation of the liquid phase (water, ethanol, toluene), the highest yield of the reaction being reached for the fibers that were swollen in water before performing the synthesis.
   - The fibers showed antimicrobial activity, especially against methicillin-resistant *Staphylococcus aureus*.

2. Design of multifunctional biomaterials based on microporous chitosan fibers functionalized by imine bond with 2-formylphenylboronic acid targeting the obtaining of wound dressings.
   - Microporous chitosan nanofibers, with average diameters less than 200 nm, inter-fibrillar pores around 1 μm and intra-fibrillar micropores up to 2 nm, were obtained by electrospinning CS/PEO mixtures, followed by removal of PEO by washing.
   - The functionalization of the fibers by imination in a heterogeneous system with 2-formylphenylboronic acid allowed the control of the degree of imination (52.8 to 14.7 %) and the fixation of imine units in the micropores or on the surface of the fibers by varying the molar ratio of the functional groups and the speed of removal of solvent from the reaction system.
   - The imination reaction was demonstrated by infrared spectroscopy, this method highlighting the vibrational band specific to newly formed imine bonds.
   - ^{1}H-NMR spectroscopy confirmed the imination reaction and allowed the quantitative evaluation of the degree of conversion of chitosan amino groups into imino units.

- The microporous nature of the fibers favored rapid swelling in water and phosphate buffer solutions of different pHs, achieving a remarkable MES around 30 g/g.
- Enzymatic biodegradation in environments of different pH, corresponding to the evolution of pH during the wound healing period, revealed an increase in biodegradation when increasing the pH to the value of 10, corresponding to the first two stages of wound healing, and rapid biodegradation in the environment of pH 5.5 characteristic of normal dermis.
- Functionalization with 2-formylphenylboronic acid gave the fibers antimicrobial activity against pathogens such as *S. aureus*, *A. brasiliensis* and *C. albicans* even for the lowest degree of imination (14.75%), correlated with the shift of the imination equilibrium towards reaction products in wet environments.
- Biocompatibility tests on normal human dermal fibroblasts indicated that the fibers can be safely used in applications involving direct contact with living tissue for a degree of imination up to 20%, while a degree of imination up to 16% determined cell adhesion and proliferation.

3. Obtaining of dressings based on chitosan mesoporous fibers loaded with a broad-spectrum antibiotic, norfloxacin, modified on the surface by imination with an aldehyde with antimicrobial activity, 2-formylphenylboronic acid.
   - Mesoporous chitosan fibers loaded with norfloxacin and coated with an antifungal agent *via* reversible imine linkages were prepared and investigated for wound healing-influencing properties.
   - The fibers were approximately 170 nm in diameter with intrafibrillar pores of approximately 2.7 nm and interfibrillar pores less than 4 μm.
   - The mesoporous nature of the fibers favored rapid swelling, reaching an equilibrium mass swelling of up to 20 g/g in less than 15 minutes, and a biodegradation percentage of up to 30% in 14 days, both processes being controlled by the pH of the medium.
   - Fibers exhibited liquid adsorption/desorption ability, indicating moisture control capability and breathability, with maximum moisture retention values up to 35%, values that meet the requirements for treating burn wounds.
   - The encapsulation of norfloxacin in the mesoporous fibers favored a slow release over time in a controlled manner.
   - The combination of chitosan, norfloxacin and the antifungal agent enriched the composite material with broad spectrum of action against Gram-negative and Gram-positive bacteria, but also against strains of fungi and yeasts.
   - The obtained materials passed the biocompatibility tests required for biomedical devices, and their subcutaneous implantation in rats did not induce harmful effects on blood, liver, and kidneys, nor allergic reactions or any immune system response. Investigation of composite materials as dressings in treatment experiments of burn wounds in rats demonstrated the benefits of this ternary composite. Mesoporous chitosan fibers favored early fibrillar synthesis, but healing was hampered by the presence of inflammatory processes. Their imination with the antifungal aldehyde significantly improved tissue regeneration. Loading the fibers with a small amount of norfloxacin followed by surface imination with the antifungal aldehyde promoted complete wound closure and tissue repair.

4. Obtaining of biomaterials based on biodegradable chitosan/trimethyl chitosan nanofibers for application as bioabsorbable dressings for wound closure and healing.
    - Defect-free CS/TMC binary mesoporous fibers were prepared with good integrity for a maximum percentage of 25% TMC, with a diameter of up to 153 nm and intrafibrillar pores with a diameter of about 3 nm, and high porosity due to the removal of poly(ethylene oxide), polymer used as co-spinning agent and sacrificial matrix.
    - The fibers showed a mass equilibrium swelling of 30 g/g in water and 15 g/g in PBS, results similar to commercial dressings used in the treatment of profusely exuding wounds.
    - CS/TMC fibers showed a degree of biodegradation of up to 45% in physiological pH in 3 days, favored by the solubility of TMC, enzymatic degradation in the presence of lysozyme (an enzyme present in biological fluids) and their mesoporous nature that favored an easy access of the solvent and of the enzyme molecules.
    - The presence of TMC significantly improved fibers' mucoadhesion due to the higher ability of permanent positive charges to interact with negatively charged mucin to form aggregates. The fibers have good bioadhesion, and easily adhere to the skin, important characteristics for implantable biomaterials.
    - The fibers are flexible and can be handled without damage, even though TMC has decreased Young's modulus causing a degree of brittleness under high force pressure. Their tensile strength value, around 10 MPa for NCT7 and NCT19, is close to that of skin tissue (2-16 MPa), indicating their utility in protecting wounds during normal patient activities.
    - The presence of TMC in the fibers endowed them with strong antimicrobial activity, especially against Gram-negative bacteria, which are the most common pathogens colonizing wounds and prolific biofilm formers.
    - Tests on normal human fibroblasts have shown that the fibers with a TMC content of less than 13% (NCT7, NCT19) can be safely used as medical devices.
    - Subcutaneous implantation of fibers in Wistar rats did not cause statistically significant deviations of biochemical parameters relevant to the clinical state and metabolic activity of organs and tissues, indicating their potential for safe in vivo use. This is an important result, considering that no *in vivo* biocompatibility tests on quaternized chitosan fibers have been reported to date.
    - CS/TMC fibers with about 13% TMC showed the best balance of properties for bioapplications, and their use in wound healing experiments proved total closure and active healing of second/third degree burn wounds in rats, with total biodegradation over 11 days, indicating the potential to function as effective bioresorbable dressings.

5. Obtaining of nanofibers based on chitosan and quaternized chitosan encapsulating copper oxide nanoparticles in order to obtain new multifunctional biomaterials.
    - Nanocomposite fibers based on a mixture of polymers (chitosan, HTCC and PEO) and different amounts of CuONPs were obtained by needle-free electrospinning using NanoSpider technology, this study reporting for the first time this type of material.
    - SEM measurements showed that CuONPs favored fibers' thinning from 270 to 126 nm.
    - Successful incorporation of CuONPs was demonstrated by EDAX and UV-vis analysis.
    - FTIR and ^{1}H-NMR spectroscopy as well as TGA analysis confirmed the presence of chitosan, quaternized chitosan and poly(ethylene oxide) and the formation of strong intermolecular forces with copper oxide nanoparticles.

- X-ray diffraction indicated the semi-crystalline nature of the fibers conferred by the phase segregation of PEO-rich crystalline domains in the semi-crystalline chitosan-rich matrix.
- CuONPs nanoparticles improved the mechanical properties of the fibers, reaching values of tensile strain up to 10 MPa and Young's modulus of 270 MPa.
- Quaternized chitosan and CuONP improved the antioxidant activity through a synergistic effect, consisting in the release of hydroxyl and amine units from the H-bond network and weakening the dissociation energy of O-H and N-H covalent bonds, making hydrogen atoms more prone to heterolytic cleavage.
- The fibers showed strong antimicrobial activity, due to quaternized chitosan and enhanced by copper oxide nanoparticles, reducing Gram-positive *S. aureus* up to 95.5 % and Gram-negative *K. pneumoniae* up to 96.2 %.
- The fibers have a good water vapor transmission rate of 750g/m^2/day, air permeability between 0.75 - 22.5 m^3/m^2 day and PM2.5 fine particle removal efficiency around 65% and PM10 around 92 %, values comparable to those of synthetic nanofibers.
- The natural origin of chitosan and quaternized chitosan resulted in approximately 40% biodegradation in 21 days and rapid fibers' degradation in soil in less than 15 days.
- All these features indicate the studied CuONPs/chitosan/quaternized chitosan/PEO nanofibers as a promising platform to develop eco materials for a wide range of applications such as dressings, masks, and air filters.

The original results presented in the thesis have been published as scientific articles in international and national ISI journals.

Papers published in ISI journals

1. **Anisiei, A.**, Bostanaru, A.-C., Mares, M. & Marin, L. (2021) Imination of chitosan nanofibers in a heterogeneous system. synthesis optimization and impact on fiber morphology. Cellulose Chemistry and Technology 55(7-8),785-793. 10.35812/CelluloseChemTechnol.2021.55.65 **F.I.= 1.3**
2. **Anisiei, A.,** Rosca, I., Sandu, A.-I., Bele, A., Cheng, X., & Marin, L. (2022) Imination of Microporous Chitosan Fibers—A Route to Biomaterials with "On Demand" Antimicrobial Activity and Biodegradation for Wound Dressings. Pharmaceutics, 14(1), 117. https://doi.org/10.3390/pharmaceutics14010117 **F.I. = 5.4**
3. **Anisiei, A.,** Oancea, F. & Marin, L. (2023) Electrospinning of chitosan-based nanofibers: from design to prospective applications. Reviews in Chemical Engineering 39 (1), 31-70. https://doi.org/10.1515/revce-2021-0003 **F.I. = 4.7**
4. **Anisiei, A.,** Andreica, B.-I., Mititelu-Tartau, L., Coman, G. C., Bilyy, R., Bila, G., Rosca, I., Sandu, A.-I., Amler, E. & Marin, L. (2023) Biodegradable trimethyl chitosan nanofiber mats by electrospinning as bioabsorbable dressings for wound closure and healing. International Journal of Biological Macromolecules 249, 126056, https://doi.org/10.1016/j.ijbiomac.2023.126056 **F.I. = 8.2**
5. Ailincai, D., Cibotaru, S., **Anisiei, A.,** Coman, C. G., Pasca, A. S., Rosca, I., ... & Marin, L. (2023). Mesoporous chitosan nanofibers loaded with norfloxacin and coated with phenylboronic acid perform as bioabsorbable active dressings to accelerate the healing of burn wounds. *Carbohydrate Polymers*, 121135. 10.1016/j.carbpol.2023.121135 **F.I. = 11.2**
6. Bejan, A., **Anisiei, A.,** Andreica, B.-I., Rosca, I., Marin, L., Chitosan nanofibers encapsulating copper oxide nanoparticles: a novel approach towards multifunctional ecological membranes with high antimicrobial and antioxidant efficiency. International Journal of Biological Macromolecules -*submitted for publication* **F.I. = 8.2**

Patent

1. „Nețesută de chitosan cu co-eliberare controlata de antibiotic si principii active," Luminita Marin, **Alexandru Anisiei**, Ailincai Daniela, Sandu Cibotaru, Bianca Andreica, Irina Rosca, No. CBI : A / 00478 / 08.08.2022

2. „Procedeu de electrofilare de nanofibre de chitosan și chitosan/chitosan cuaternizat," Luminita Marin, **Alexandru Anisiei**, Bianca Andreica, Liliana Mititelu Tarțău, No. CBI : A / 00749 / 21.11.2022

Proceeding works

1. **Anisiei, A**., Rosca, I. & Marin, L. (2020) Functionalized Chitosan Nanofibers with Enhanced Antimicrobial Activity for Burn Wound Healing Applications. Proceedings of the First International Conference on "Green" Polymer Materials, doi:10.3390/CGPM2020-07216

Papers published in ISI-rated journals (results not included in the thesis)

1. Marin, L., Popa, M., **Anisiei, A**., Irimiciuc, S.-A., Agop, M., Petrescu, T.-C., Vasincu, D., & Himiniuc, L. (2021). A Theoretical Model for Release Dynamics of an Antifungal Agent Covalently Bonded to the Chitosan. Molecules, 26(7), 2089. https://doi.org/10.3390/molecules26072089 **F.I. = 4.6**
2. Lungu, R., **Anisiei, A**., Rosca, I., Sandu, A.-I., Ailincai, D., & Marin, L. (2021). Double functionalization of chitosan-based nanofibers towards biomaterials for wound healing. Reactive and Functional Polymers, 167, 105028. https://doi.org/10.1016/j.reactfunctpolym.2021.105028 **F.I. = 5.1**
3. Serbezeanu, D., Vlad-Bubulac, T., Onofrei, M. D., Doroftei, F., Hamciuc, C., Ipate, A.-M., **Anisiei, A**., Lisa, G., Anghel, I., Șofran, I.-E., & Popescu, V. (2022). Phosphorylated Poly(vinyl alcohol) Electrospun Mats for Protective Equipment Applications. Nanomaterials, 12(15), 2685. https://doi.org/10.3390/nano12152685 **F.I. = 5.3**
4. Andreica, B.-I., **Anisiei, A**., Rosca, I., Sandu, A.-I., Pasca, A. S., Tartau, L. M., & Marin, L. (2023). Quaternized chitosan/chitosan nanofibrous mats: An approach toward bioactive materials for tissue engineering and regenerative medicine. Carbohydrate Polymers, 302, 120431. https://doi.org/10.1016/j.carbpol.2022.120431 **F.I. = 11.2.**
5. Marin, L., Andreica, B.-I., **Anisiei, A.**, Cibotaru, S., Bardosova, M., Materon, E. M., & Oliveira, O. N. (2023). Quaternized chitosan (nano)fibers: A journey from preparation to high performance applications. *International Journal of Biological Macromolecules*, *242*, 125136. https://doi.org/10.1016/j.ijbiomac.2023.125136 **F.I. = 8.2**
6. Andreica, B.-I., **Anisiei, A.**, Iftime, M., Ababei, R.-V., Ochiuz, L., Vasincu, D., Vasilache, I.-A., Volovat, C., Boboc D., Poroch, V., Eva, L., Agop, M., Scripcariu, D.-V., Volovat S.R., Swelling and biodegradation profile of chitosan/quaternized chitosan nanofibers in media mimicking wound exudate. A theoretical model – experimental approach, Pharmaceutics -*submitted for publication* **F.I. = 8.2**

The PhD student thanks the following projects for their support:

1. Eco-nanomaterials based on chitosan for applications of contemporary interest (ECO-MAT), PN-III-P4-ID-PCE-2020-2717
2. Resorbable bandage with controlled release of norfloxacin for healing burns (BurnHeal), PN-III-P2-2.1-PED-2019-5071
3. Dressings for intelligent wound healing (SWORD), PN-III-P3-3.6-H2020-2020-0138

4. Smart Wound Monitoring Restorative Dressings (SWORD), H2020-MSCA-RISE-2019: (no. 873123)
5. Innovative Electrospun Membranes based on Phosphorus-containing Polymers for Protective Clothing (InElPHoPRo), PN-III-P1-1.1-TE-2019-0639
6. New "green" technology for advanced water treatment based on functionalized polysulfones/ionic liquids membranes (GreenTechMembr), PN-III-P2-2.1-PED-2019-301

Participation in national and international scientific sessions

Oral communications

1. **Anisiei, A**., Rosca, I., Marin, L. (2020) Iminoboronate-chitosan nanofibers with antimicrobial activity for burn wound healing applications, Open door to the future scientific communications of young researchers MacroYouth, Iasi, Romania.
2. **Anisiei, A**., Rosca, I., Marin, L. (2020) Functionalized chitosan nanofibers with enhanced antimicrobial activity for burn wound healing applications The First International Conference on "Green" Polymer Materials.
3. **Anisiei, A**., Rosca, I., Sandu, A.-I., Bele, A., Marin, L. (2021) Biodegradable imino-chitosan nanofibers as wound dressing materials MacroYouth Open door to the future scientific communications of young researchers MacroYouth Second Edition Iasi, Romania.
4. **Anisiei, A**., Andreica, B.-I., Marin, L. (2022) Chitosan based nanofibers for wound dressing applications XXXIInd edition of the International Congress of "Apollonia" University of Iasi, Iasi, Romania.
5. **Anisiei, A.**, Andreica, B.-I., Marin, L. (2022) Biodegradable chitosan/quaternized chitosan nanofibers as wound dressings 12th International Conference On Materials Science & Engineering (BRAMAT), Brasov, Romania.
6. Cibotaru S., Ailincai D., **Anisiei A.**, Marin L. (2022) Bandages based on chitosan nanofibers for burn healing applications, 12th International Conference on Materials Science and Engineering, Brasov, Romania.
7. Marin L., Ailincai D., Iftime M.-M., Craciun A.-M., Bejan A., **Anisiei A.**, Andreica B.-I. (2022) Chitosan imination: an opportunity towards biomaterials with broad application spectrum, 7th International Congress on Biomaterials and Biosensors (BIOMATSEN 2022), Muğla, Turkey.
8. Marin L., Ailincai D., Cibotaru S., **Anisiei A.**, Rosca I., Mititelu-Tartau L. (2022) Biodegradable chitosan-based nanofibers with broad spectrum antimicrobial activity for wound healing applications, EPF European Polymer Federation, Prague, Czech Republic.
9. Marin L, **Anisiei A**., Andreica B.I., Mititelu-Tartau L., Coman C., Bilyy R., Bila G., Rosca I., Sandu A.I., Amler E. (2023) Quaternized chitosan-based nanofibers as bioabsorbable wound dressings, The 14th International Conference of the European Chitin Society (EUCHIS 2023) and the 15th International Conference on Chitin and Chitosan (15th ICCC), Siglufjörður, Iceland
10. Bejan A., Anisiei A., Marin L. (2023) Chitosan/quaternized chitosan – based nanofibers mesh as promising materials for air filtration, The 14th International Conference of the European Chitin Society (EUCHIS 2023) and the 15th International Conference on Chitin and Chitosan (15th ICCC), Siglufjörður, Iceland
11. **Anisiei A.**, Bejan A., Marin L. (2023) Copper oxide nanoparticle-doped nanofiber mats for effective air filtration, 8th EPNOE International Polysaccharides Conference, Graz, Austria.

12. Marin L, **Anisiei A**., Andreica B.I., Mititelu-Tartau L., Coman C., Bilyy R., Bila G., Rosca I., Sandu A.I, Amler E. (2023) Nanofibers based on quaternized chitosan as bioabsorbable wound dressings, 8th EPNOE International Polysaccharides Conference, Graz, Austria.
13. Ailincai D., Cibotaru S., **Anisiei A.**, Rosca I., Mititelu-Tartau L., Marin L. (2023) Chitosan nanofibers for burn healing applications, 8th EPNOE International Polysaccharides Conference, Graz, Austria.

Poster presentation

1. **Anisiei, A.**, Andreica, B.-I., Marin, L., (2022) Electrospinning of chitosan/quaternary salts of chitosan nanofibers for biomedical application. EPF European Polymer Congress, Prague, Czech Republic.
2. **Anisiei, A.**, Rosca, I., Sandu, A.-I., Bele, A., Marin, L., (2022) Imination of chitosan fibers towards potential antimicrobial wound dressings EPF European Polymer Congress, Prague, Czech Republic.
3. Lungu R., **Anisiei A.**, Rosca I., Sandu A.-I, Ailincai D., Marin L., (2021) Double-functionalized chitosan nanofibers for wound healing, Progress in Organic and Macromolecular Compounds, 28th Edition, Iasi, Romania
4. Cibotaru S., Ailincai D., **Anisiei A.**, Marin L., (2022) Drug delivery systems based on imino-chitosan nanofibers for burn healing applications, EPF European Polymer Federation 2022, Prague, Czech Republic.
5. Andreica B.-I., **Anisiei A**., Rosca I., Sandu A.-I., Mititelu-Tartau L., Marin L. (2023) Chitosan/quaternized chitosan nanofibers designed for biomedical applications, 8th EPNOE International Polysaccharides Conference, Graz, Austria.
6. **Anisiei A**., Bejan A., Cibotaru S., Marin L. (2023) Quaternized chitosan nanofibers for bone regeneration, 8th EPNOE International Polysaccharides Conference, Graz, Austria.

Selected bibliography:

[1] R.C. Goy, D. de Britto, O.B.G. Assis, Polímeros 19 (2009) 241–247.
[2] A. Anisiei, I. Rosca, A.-I. Sandu, A. Bele, X. Cheng, L. Marin, Pharmaceutics 14 (2022) 117.
[3] R. Lungu, A. Anisiei, I. Rosca, A.-I. Sandu, D. Ailincai, L. Marin, React Funct Polym 167 (2021) 105028.
[4] L. Marin, B. Dragoi, N. Olaru, E. Perju, A. Coroaba, F. Doroftei, G. Scavia, S. Destri, S. Zappia, W. Porzio, Eur Polym J 120 (2019) 109214.
[5] L. Marin, D. Ailincai, M. Mares, E. Paslaru, M. Cristea, V. Nica, B.C. Simionescu, Carbohydr Polym 117 (2015) 762–770.
[6] L. Marin, A. Anisiei, D. Ailincai, S. Cibotaru, B.-I. Andreica, I. Rosca, Chitosan Non-Woven Mat with Co-Delivery of Antibiotic and Active Principles, 2022.
[7] A. Anisiei, F. Oancea, L. Marin, Reviews in Chemical Engineering 39 (2023) 31–70.
[8] S. Guo, Y. Ren, R. Chang, Y. He, D. Zhang, F. Guan, M. Yao, ACS Appl Mater Interfaces 14 (2022) 34455–34469.
[9] H. Xue, Z. Zhang, Z. Lin, J. Su, A.C. Panayi, Y. Xiong, L. Hu, Y. Hu, L. Chen, C. Yan, X. Xie, Y. Shi, W. Zhou, B. Mi, G. Liu, Bioact Mater 18 (2022) 552–568.
[10] B.-I. Andreica, X. Cheng, L. Marin, Eur Polym J 139 (2020) 110016.
[11] ISO 10993-5:2009(en), (2009).
[12] G. Silva-Santana, J.C. Bax, D.C.S. Fernandes, D.T.L. Bacellar, C. Hooper, A.A.S.O. Dias, C.B. Silva, A.M. de Souza, S. Ramos, R.A. Santos, T.R. Pinto, M.A. Ramão, A.L. Mattos-Guaraldi, Animal Model Exp Med 3 (2020) 304–315.
[13] K. Satoh, J.E. Poelma, L.M. Campos, B. Stahl, C.J. Hawker, Polym. Chem. 3 (2012) 1890–1898.
[14] B.-I. Andreica, A. Anisiei, I. Rosca, A.-I. Sandu, A.S. Pasca, L.M. Tartau, L. Marin, Carbohydr Polym 302 (2023) 120431.
[15] S. Yang, Z. Liu, Y. Liu, Y. Jiao, J Mater Sci 50 (2015) 1544–1552.
[16] H.M. Alhusaiki Alghamdi, Opt Mater (Amst) 134 (2022) 113101.
[17] D. Renuga, J. Jeyasundari, A.S. Shakthi Athithan, Y. Brightson Arul Jacob, Mater Res Express 7 (2020) 045007.
[18] D. Raj Preeth, M. Shairam, N. Suganya, R. Hootan, R. Kartik, K. Pierre, C. Suvro, S. Rajalakshmi, JBIC Journal of Biological Inorganic Chemistry 24 (2019) 633–645.
[19] K. Dulta, G. Koşarsoy Ağçeli, P. Chauhan, R. Jasrotia, P.K. Chauhan, J.O. Ighalo, Sustainable Environment Research 32 (2022) 2.
[20] S. Kumar, J. Koh, Int J Mol Sci 13 (2012) 6102–6116.
[21] Y. Kong, W. Zhang, T. He, X. Yang, W. Bi, J. Li, W. Yang, W. Chen, Carbohydr Polym 304 (2023) 120485.
[22] R. Nawalakhe, Q. Shi, N. Vitchuli, J. Noar, J.M. Caldwell, F. Breidt, M.A. Bourham, X. Zhang, M.G. McCord, J Appl Polym Sci 129 (2013) 916–923.
[23] A. Nazir, N. Khenoussi, T. Hussain, S. Abid, L. Schacher, D. Adolphe, A. Zahir, M.B. Qadir, Z. Khaliq, A. Shahzad, Polymer Bulletin 77 (2020) 5155–5173.
[24] C. Akduman, N. Oglakcıoglu, A. Kumbasar PA, B. Sarı, Journal of Fashion Technology & Textile Engineering s4 (2018).
[25] M.M. Iftime, G.L. Ailiesei, E. Ungureanu, L. Marin, Carbohydr Polym 223 (2019) 115040.